

Critical temperature of triplet superconductor-ferromagnet bilayers as a probe for pairing symmetry

Erik Wegner Hodt,¹ Carla Cirillo,² Angelo Di Bernardo,³ Carmine Attanasio,³ and Jacob Linder¹

¹*Center for Quantum Spintronics, Department of Physics, Norwegian University of Science and Technology, NO-7491 Trondheim, Norway*

²*CNR-SPIN, c/o Università degli Studi di Salerno - Via Giovanni Paolo II, 132 - I-84084 - Fisciano (Sa), Italy*

³*Dipartimento di Fisica "E.R. Caianiello", Università degli Studi di Salerno - Via Giovanni Paolo II, 132 - I-84084 - Fisciano (Sa), Italy*

(Dated: February 19, 2024)

Identifying superconducting materials with spin-polarized Cooper pairs is an important objective both for exploration of new fundamental physics and for cryogenic applications in spintronics and quantum sensing. We here compute the critical temperature T_c of the superconducting transition in a bilayer comprised of a superconductor with an intrinsic spin-triplet order parameter and a ferromagnet. We determine how T_c varies both with the thickness of the ferromagnet and its magnetization direction. We show that both the orbital and spin part of the triplet superconducting order parameter leave clear signatures in T_c which do not appear in a bilayer of a conventional s -wave superconductor and a ferromagnet. In particular, the dependence of T_c on these variables changes depending on whether or not the superconducting order parameter features Andreev bound-states and also changes qualitatively when the magnetization is rotated in the plane of the ferromagnetic film. Measurements of T_c in such bilayers are therefore useful to identify the pairing symmetry of intrinsic triplet superconductors.

I. INTRODUCTION

Merging materials with fundamentally different properties can give rise to new quantum physics at the interface which is interesting both from a fundamental perspective and in terms of possible applications. A prime example of this is superconducting and magnetic materials, a combination which has been studied thoroughly in particular during the last decades [1, 2].

The most fundamental property of superconductors is the Meissner effect, leading to expulsion of magnetic fields. Notwithstanding, it is possible for magnetic order and superconductivity to coexist in hybrid structures. The Cooper pairs in superconductors can align their spins to endure the spin-polarized environment provided by ferromagnets, opening the possibility to have dissipationless transport not only of charge, but also of spin. Spin-polarized superconductivity, known as triplet pairing, is well-established in heterostructures comprised of superconductors and ferromagnets [2–8]. Intrinsic triplet superconducting materials are, however, scarce. It has been experimentally established that uranium-based ferromagnetic superconductors such as UGe_2 and URhGe feature triplet pairing [9–12], but besides these evidence for intrinsic triplet pairing in superconducting materials is mostly inconclusive.

Triplet pairing can be put on firm experimental ground by performing measurements of multiple physical observables if all such measurements indicate the presence of spin-polarized superconductivity. It is therefore important to establish how triplet pairing is manifested in various experimentally accessible quantities. The critical temperature T_c at which a material enters its superconducting phase is both a fundamental and one of the most accessible experimental quantities available.

Motivated by this, we here report a theoretical study of how T_c in a triplet superconductor is altered when placing the superconductor in contact with a ferromagnet. Such a setup, with a conventional s -wave superconductor described by Bardeen-Cooper-Schrieffer (BCS) theory rather than a triplet superconductor, has been experimentally demonstrated to yield clear evidence of proximity-induced triplet pairing [13–16].

Here, we instead investigate how T_c of intrinsically present triplet Cooper pairs changes when introduced to a ferromagnetic environment. We find that measurements of T_c provides clear information about the nature of the superconducting triplet state. Specifically, the behavior of T_c in the presence of a ferromagnet reveals information about both the orbital part and the spin part of the triplet pairing state. We therefore argue that T_c measurements of candidate triplet superconducting materials placed in contact with conventional ferromagnets are a useful tool to infer information about the properties of the superconducting state and obtain evidence supporting the spin-triplet nature of the order parameter.

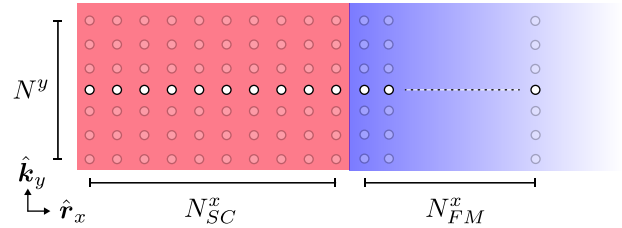


FIG. 1. The bilayer geometry consisting of a p-wave triplet superconductor (red) adjacent to a ferromagnetic layer (blue) of varying thickness. The system is assumed periodic in the y -direction parallel to the interface and of finite size in the x -direction normal to the interface. It is thus suitable to describe the system with real-space coordinates r_x in x and momentum-space coordinates k_y in y . N^y denotes the number of momentum modes in y while N_{SC}^x and N_{FM}^x denote the number of x -direction lattice sites in the SC and FM, respectively.

II. MODEL

We consider a tight binding Hamiltonian on a square lattice bilayer structure consisting of a superconductor (SC) and an adjacent ferromagnet (FM). In the SC, we consider nearest

neighbour attractive electron-electron interaction,

$$H_{SC} = - \sum_{\langle i,j \rangle, \sigma} t_{ij} c_{i,\sigma}^\dagger c_{j,\sigma} - \sum_{i,\sigma} \mu c_{i,\sigma}^\dagger c_{i,\sigma} + \sum_{\langle i,j \rangle, \sigma} V_{ij} n_{i,\sigma} n_{j,\sigma} \quad (1)$$

where $c_{i,\sigma}^\dagger$ ($c_{i,\sigma}$) creates (annihilates) an electron with spin σ on site i , $\langle i, j \rangle$ denotes all nearest neighbor site pairs, and μ is the chemical potential. We shall assume the hopping to be isotropic in the following, $t_{ij} = t > 0$. $V_{ij} \leq 0$ is the coupling strength of an effective, attractive electron-electron interaction in the system, On account of being a nearest-neighbor interaction, it can give rise to p -wave superconductivity.

Adjacent to the superconductor, we consider a ferromagnet modelled by the following Hamiltonian

$$H_{FM} = - \sum_{\langle i,j \rangle, \sigma} t c_{i,\sigma}^\dagger c_{j,\sigma} - \sum_{i,\sigma} \mu c_{i,\sigma}^\dagger c_{i,\sigma} - m \sum_{i,\sigma,\sigma'} \hat{\mathbf{n}} \cdot \boldsymbol{\sigma} c_{i,\sigma}^\dagger c_{i,\sigma'} \quad (2)$$

where m is the strength of the FM exchange field, $\hat{\mathbf{n}}$ is a unit vector denoting the FM magnetization direction, and $\boldsymbol{\sigma}$ is the vector of Pauli matrices. The SC and FM regions are connected by electron hopping, enabling a proximity effect between the materials, but the attractive electron-electron pairing strength V_{ij} is zero in the FM while the strength of the FM exchange field m is zero in the SC. We will for simplicity only consider the case where the chemical potential is constant across the heterostructure.

A. Constructing the Hamiltonian matrix

We shall assume the system to be periodic in y , the direction parallel to the interface. In order to take advantage of this periodicity, we introduce momentum-space operators in the y -direction as indicated by the system geometry presented in Fig. 1. Given the Fourier-transformed operators,

$$c_{(i_x, i_y), \sigma} = \frac{1}{\sqrt{N_y}} \sum_{k_y} c_{i_x, k_y, \sigma} e^{ik_y r_y} \quad (3)$$

$$c_{(i_x, i_y), \sigma}^\dagger = \frac{1}{\sqrt{N_y}} \sum_{k_y} c_{i_x, k_y, \sigma}^\dagger e^{-ik_y r_y},$$

the Hamiltonian, now block-diagonal in k_y modes, can be written as

$$H = E_0 + \frac{1}{2} \sum_{k_y} B_{k_y}^\dagger H_{k_y} B_{k_y} \quad (4)$$

where the operator-independent energy E_0 gives a contribution to the total system energy which is not relevant for this paper.

Each k_y block in the total Hamiltonian matrix (Eq. (4)) is now a $4N_{SC}^x N_{FM}^x \times 4N_{SC}^x N_{FM}^x$ matrix given by

$$B_{k_y}^\dagger H_{k_y} B_{k_y} = \sum_{\langle i_x, j_x \rangle} (W_{i_x}^{k_y})^\dagger h_{i_x, j_x}^{k_y} W_{j_x}^{k_y} \quad (5)$$

where the sum over i_x, j_x runs over the 1D string of lattice sites in the SC and FM. We shall from now on omit subscripts on real-space and momentum indices, taking a real space coordinate i to implicitly mean a site in the x direction and vice versa for momentum indices. The basis vectors W_i^k are given by

$$W_i^k = \left(c_{i,k,\uparrow} \quad c_{i,k,\downarrow} \quad c_{i,-k,\uparrow}^\dagger \quad c_{i,-k,\downarrow}^\dagger \right)^T \quad (6)$$

When i, j are in the SC, the matrix elements $h_{i,j}^k$ are defined for $i = j$ as (see appx. A for details)

$$h_{i,i}^{k,SC} = \begin{bmatrix} \varepsilon_{k_y} + \mu & 0 & -2\Delta_{i,k}^{\uparrow,\hat{y}} & 0 \\ 0 & \varepsilon_k + \mu & 0 & -2\Delta_{i,k}^{\downarrow,\hat{y}} \\ -2(\Delta_{i,k}^{\uparrow,\hat{y}})^\dagger & 0 & -(\varepsilon_k + \mu) & 0 \\ 0 & -2(\Delta_{i,k}^{\downarrow,\hat{y}})^\dagger & 0 & -(\varepsilon_k + \mu) \end{bmatrix} \quad (7)$$

and for $j = i \pm \hat{x}$,

$$h_{i,i \pm \hat{x}}^{k,SC} = \begin{bmatrix} -t & 0 & -2\Delta_i^{\uparrow,\pm\hat{x}} & 0 \\ 0 & -t & 0 & -2\Delta_i^{\downarrow,\pm\hat{x}} \\ 2(\Delta_i^{\uparrow,\pm\hat{x}})^\dagger & 0 & t & 0 \\ 0 & 2(\Delta_i^{\downarrow,\pm\hat{x}})^\dagger & 0 & t \end{bmatrix} \quad (8)$$

Here we have defined the order parameters (also known as gaps in the context of superconductivity)

$$\Delta_i^{\sigma,\pm\hat{x}} = \frac{V_x}{N_y} \sum_{k'} F_{i,k'}^{\sigma,\pm\hat{x}} \quad (9)$$

$$\Delta_{i,k}^{\sigma,\hat{y}} = \frac{V_y}{N_y} \sum_{k'} 2 \cos(k' - k) F_{i,k'}^{\sigma,\hat{y}} \quad (10)$$

the pairing amplitudes

$$F_{i,k'}^{\sigma,\pm\hat{x}} = \langle c_{i,k',\sigma} c_{i \pm \hat{x}, -k', \sigma} \rangle \quad (11)$$

$$F_{i,k'}^{\sigma,\hat{y}} = \langle c_{i,k',\sigma} c_{i, -k', \sigma} \rangle, \quad (12)$$

and the y -direction dispersion

$$\varepsilon_k = -2t \cos k - \mu \quad (13)$$

The matrix elements for the FM is given similarly for $i = j$ in the FM as

$$h_{i,i}^{FM} = \begin{bmatrix} \varepsilon_k + h^{\uparrow\uparrow} & h^{\uparrow\downarrow} & 0 & 0 \\ h^{\downarrow\uparrow} & \varepsilon_k + h^{\downarrow\downarrow} & 0 & 0 \\ 0 & 0 & -(\varepsilon_k + h^{\uparrow\uparrow}) & -(h^{\uparrow\downarrow})^* \\ 0 & 0 & -(h^{\downarrow\uparrow})^* & -(\varepsilon_k + h^{\downarrow\downarrow}) \end{bmatrix} \quad (14)$$

where we have defined the short-hand matrix $h = m \hat{\mathbf{n}} \cdot \boldsymbol{\sigma}$. For $j = i \pm \hat{x}$, we have

$$h_{i,i \pm \hat{x}}^{FM} = \begin{bmatrix} -t & 0 & 0 & 0 \\ 0 & -t & 0 & 0 \\ 0 & 0 & t & 0 \\ 0 & 0 & 0 & t \end{bmatrix} \quad (15)$$

B. Diagonalizing the Hamiltonian

As the Hamiltonian is diagonal in k , we can diagonalize the k blocks of the Hamiltonian individually, allowing us to access significantly larger system sizes than in the case of real-space coordinates in two dimensions. Starting from Eq. (4), it follows that we can write the matrix block $H_k = U_k \Lambda_k U_k^\dagger$ where the eigenvectors of H_k ,

$$\Phi_{n,k} = [\varphi_{n,1,k} \ \dots \ \varphi_{n,i,k} \ \dots \ \varphi_{n,N,k}]^T \quad (16)$$

$$\varphi_{n,i,k} = [u_{n,i,k} \ v_{n,i,k} \ x_{n,i,k} \ w_{n,i,k}]$$

are the columns of U_k ,

$$U_k = [\Phi_1 \ \Phi_2 \ \dots \ \Phi_{4N}] \quad (17)$$

and where $N = N_{SC}^x N_{FM}^x$. Using the unitary matrices U_k , we may now diagonalize the H_k block,

$$H = E_0 + \frac{1}{2} \sum_k \Gamma_k^\dagger \Lambda_k \Gamma_k \quad (18)$$

$$= E_0 + \frac{1}{2} \sum_k E_{n,k} \gamma_{n,k}^\dagger \gamma_{n,k} \quad (19)$$

where we have introduced the new Bogoliubov operators

$$\Gamma_k = U_k^\dagger B_k \Rightarrow B_k = U_k \Gamma_k \quad (20)$$

and where $\Gamma_k = [\gamma_{1,k} \ \gamma_{2,k} \ \dots \ \gamma_{4N,k}]^T$. Using Eq. (20), we can express the original fermion operators in terms of the new Bogoliubov operators,

$$c_{i,k,\uparrow} = \sum_{n=1}^{4N} u_{n,i,k} \gamma_{n,k}, \quad c_{i,k,\downarrow} = \sum_{n=1}^{4N} v_{n,i,k} \gamma_{n,k} \quad (21)$$

$$c_{i,-k,\uparrow}^\dagger = \sum_{n=1}^{4N} w_{n,i,k} \gamma_{n,k}, \quad c_{i,-k,\downarrow}^\dagger = \sum_{n=1}^{4N} x_{n,i,k} \gamma_{n,k}$$

There are $4N$ operators in the Hamiltonian, but only $2N$ are independent. To regain the correct number of degrees of freedom, we proceed by using that positive and negative momentum operators and eigenvalues are related by the following relations,

$$\gamma_{n,k} = \gamma_{n,-k}^\dagger, \quad E_{n,k} = -E_{n,-k} \quad (22)$$

In order to incorporate this dependence between operators, we split the sum over momentum modes in the diagonalized Hamiltonian (Eq. (19)) into three parts, $k > 0$, $k = 0$ and $k < 0$, and rewrite it as a sum over only $k = 0$ and $k > 0$ modes, making use of the above relations. The Hamiltonian expressed in terms of independent operators γ/γ^\dagger then becomes

$$H = E_0 + \frac{1}{2} \sum_{n,k>0} E_{n,k} + \frac{1}{2} \sum_{E_{n,0} \geq 0} E_{n,0} + \sum_{n,k>0} E_{n,k} \gamma_{n,k}^\dagger \gamma_{n,k} + \sum_{E_{n,0} \geq 0} E_{n,0} \gamma_{n,0}^\dagger \gamma_{n,0} \quad (23)$$

The self-consistent expressions for the gaps are now obtained by using the transformed operators from Eq. (21) in the pairing amplitude expressions from Eq. (10),

$$F_{i,k}^{\uparrow,\pm\hat{x}} = \frac{1}{N^y} \left(\sum_{k'>0,n} \left[(w_{n,i,k'}^* u_{n,i\pm\hat{x},k'} - u_{n,i,k'} w_{n,i\pm\hat{x},k'}^*) f(E_{n,k'}) + u_{n,i,k'} w_{n,i\pm\hat{x},k'}^* \right] \right. \\ \left. + \sum_{E_{n,0} \geq 0} \left[(w_{n,i,0}^* u_{n,i\pm\hat{x},0} - u_{n,i,0} w_{n,i\pm\hat{x},0}^*) f(E_{n,0}) + u_{n,i,0} w_{n,i\pm\hat{x},0}^* \right] \right) \quad (24)$$

$$F_{i,k}^{\downarrow,\pm\hat{x}} = \frac{1}{N^y} \left(\sum_{k'>0,n} \left[(x_{n,i,k'}^* v_{n,i\pm\hat{x},k'} - v_{n,i,k'} x_{n,i\pm\hat{x},k'}^*) f(E_{n,k'}) + v_{n,i,k'} x_{n,i\pm\hat{x},k'}^* \right] \right. \\ \left. + \sum_{E_{n,0} \geq 0} \left[(x_{n,i,0}^* v_{n,i\pm\hat{x},0} - v_{n,i,0} x_{n,i\pm\hat{x},0}^*) f(E_{n,0}) + v_{n,i,0} x_{n,i\pm\hat{x},0}^* \right] \right) \quad (25)$$

$$F_{i,k}^{\uparrow,\hat{y}} = \frac{2}{N^y} \left(\sum_{k'>0} \left[(\cos(-k' - k) w_{n,i,k'}^* u_{n,i,k'} - \cos(k' - k) u_{n,i,k'} w_{n,i,k'}^*) f(E_{n,k'}) \right. \right. \\ \left. \left. + \cos(k' - k) u_{n,i,k'} w_{n,i,k'}^* \right] + \sum_{E_{n,0} \geq 0} \cos(k) u_{n,i,0} w_{n,i,0}^* \right) \quad (26)$$

$$F_{i,k}^{\downarrow,\hat{y}} = \frac{2}{N^y} \left(\sum_{k' > 0} \left[(\cos(-k' - k)x_{n,i,k'}^* v_{n,i,k'} - \cos(k' - k)v_{n,i,k'} x_{n,i,k'}^*) f(E_{n,k'}) \right. \right. \\ \left. \left. + \cos(k' - k)v_{n,i,k'} x_{n,i,k'}^* \right] + \sum_{E_{n,0} \geq 0} \cos(k)v_{n,i,0} x_{n,i,0}^* \right) \quad (27)$$

In order to characterize the effect of the adjacent FM on the superconductivity in the SC, we will consider the local density of states (LDOS) $N_i(E)$ on the lattice. To obtain an expression for the LDOS, we note that the number of charges at all sites with lattice index $i = i_x$ in the x -direction can be obtained by summing over all corresponding sites in the y -direction. In effect, we will consider

$$\rho_i = \sum_{i_y, \sigma} \rho_{i,i_y} = \sum_{\sigma} \sum_k \langle c_{i,k,\sigma}^\dagger c_{i,k,\sigma} \rangle \quad (28)$$

where we have transformed to the momentum-description in the y direction. To obtain an analytic expression for $N_i(E)$, we use that the charge number at site i as given above is defined by an energy integral of $N_i(E)$ weighted by the Fermi-Dirac distribution function $f(E)$,

$$\rho_i = \sum_k \sum_{\sigma} \langle c_{i,k,\sigma}^\dagger c_{i,k,\sigma} \rangle = \int_{-\infty}^{\infty} dE N_i(E) f(E) \quad (29)$$

Comparing the two formulations for the charge number ρ_i and using the relation between the positive and negative momentum operators discussed above, the LDOS may be written as

$$N_i(E) = \sum_{k > 0, n} \left[(|u_{n,i,k}|^2 + |v_{n,i,k}|^2) \delta(E - E_{n,k}) \right. \\ \left. + (|w_{n,i,k}|^2 + |x_{n,i,k}|^2) \delta(E + E_{n,k}) \right] \\ + \sum_{E_{n,0} \geq 0, n} \left[(|u_{n,i,0}|^2 + |v_{n,i,0}|^2) \delta(E - E_{n,0}) \right. \\ \left. + (|w_{n,i,0}|^2 + |x_{n,i,0}|^2) \delta(E + E_{n,0}) \right] \quad (30)$$

C. Binary search algorithm

In order to obtain an estimate for T_c of the SC/FM bilayer we utilize a binary search algorithm [17, 18]. The usual self-consistency scheme would entail obtaining a self-consistent gap for all temperatures within a range $[T_{min}, T_{max}]$ and estimating T_c as the temperature at which the gap crosses above a predetermined threshold. If we for instance denote a self-consistent solution to either of the gaps from Eq. 10 obtained at $T = 0$ as Δ_0 , then the T_c threshold could be the temperature at which the gap falls below $\Delta_0/1000$. An accurate estimate for T_c is computationally expensive with this approach. Instead, we perform a binary search algorithm where only a handful of self-consistent iterations are performed for each parameter configuration.

To obtain an estimate for T_c , we proceed in the following way: one first obtains the fully self-consistent $T = 0$ gap

Δ_0 for a temperature well below T_c , denoted T_{min} . Based on the system parameters, one can then select a T_{max} well above T_c and discretize the range $[T_{min}, T_{max}]$ into a given number of discrete temperature steps, defining a range in which T_c is expected to be. A binary search is now performed on this temperature range, using a small fraction $\Delta_0/1000$ of the self-consistent solution as the initial value of the gap. After n iterations ($n = 10$ in calculations presented in this paper), a check is performed in order to determine whether the gap has increased above $\Delta_0/1000$, implying that we are below T_c , or decreased below Δ_0 , implying that we are above T_c . The temperature value at which the binary search algorithm converges is our estimate for the critical temperature. As probe for the gap magnitude, the superconducting gap at a site in the middle of the SC is used.

III. RESULTS AND DISCUSSION

The normalized critical temperature T_c for the SC/FM bilayer structure as a function of FM thickness depends on both the orbital and spin part of the superconducting order parameter as shown in Fig. (2) for a system consisting of 30 real-space sites in the SC and 0-30 real-space sites in the FM. In the figures, $T_{c,0}$ is the critical temperature of the superconductor when it is not in proximity to any material. The number of momentum modes was $N^y = 121$ and an attractive interaction strength of $V_x = V_y = -0.85t$ was used. For the chosen parameters, the superconducting coherence length ξ is estimated to be approximately 10 sites for p_y pairing and around 15 sites in the case of p_x pairing. ξ is estimated by a visual inspection of the gap magnitude in the SC interior, see Fig. 3. The superconducting region of our system is thus 2-3 ξ thick in the direction normal to the interface. A chemical potential of $\mu = -0.5t$ was used to distinguish between spin-up and -down behaviour as the FM density-of-states (DOS) is spin-degenerate at the Fermi level independent of exchange field strength if one sets $\mu = 0.0$. The (a) subfigure shows the normalized T_c in the case of p_y pairing. i.e. pairing parallel to the SC/FM interface, while (b) presents the same results for p_x pairing normal to the interface, both for the normal metal case as well as FM magnetized in y and z direction. For the spin-structure of the pairing considered in this paper, magnetization in z and x are equivalent. This can be understood in terms of the triplet \mathbf{d} -vector [19] which for the superconducting pairing considered here has zero x and z components. We considered FM exchange field strengths ranging between $0.1 - 1.0t$. In the presentation of the results, given below, we will also compare T_c in the triplet SC/FM case with T_c in a triplet SC/NM case for a more complete understanding of the physics.

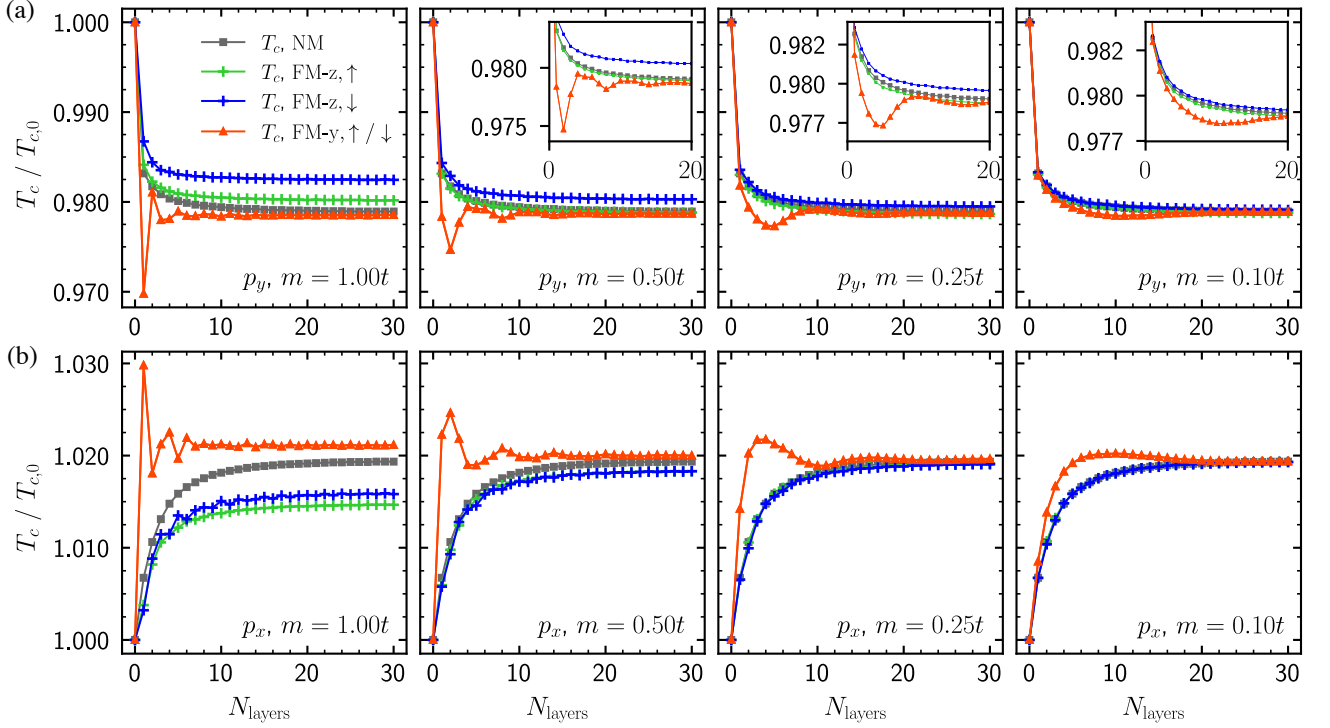


FIG. 2. Normalized critical temperature T_c is shown as function of number of NM/FM layers for p_x - and p_y -type pairing for a pairing strength $V_x = V_y = -0.85t$. The system considered consists of $N_{SC}^x = 30$ sites in the superconductor and $N^y = 121$ momentum modes in the y -direction. Using a simple estimate for the superconducting coherence length ξ (see Fig. 3), the size of the superconducting region corresponds to 2-3 ξ along the direction normal to the interface. (a) For p_y pairing, we observe T_c exponentially decaying with added NM layers. For FM, we observe an oscillatory T_c behaviour for FM polarized in y while the z polarized FM shows a NM-like decay, but which converges to a shifted, spin-dependent critical temperature. (b) For p_x pairing, we predict an increase in T_c for both FM and NM layers. For FM polarized in y , T_c is observed to oscillate as function of layer number with an oscillation frequency decreasing with exchange field strength. The FM polarized in z shows a near monotonous decay, resembling the normal metal case, but with a similarly shifted asymptotic T_c as for p_y pairing. The general increase in T_c with the addition of layers is generally attributed to a decrease in the suppressive effect of Andreev bound states on the gap in the SC. The insets in the top row show a zoom-in of each panel.

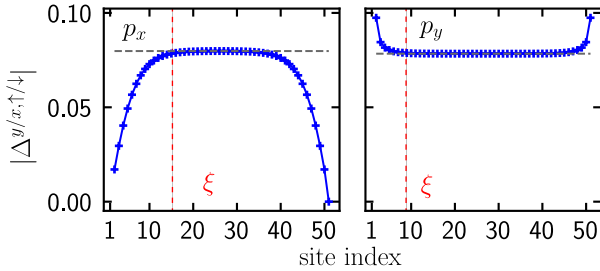


FIG. 3. The spatial dependence of the SC gap is shown for a bare SC with $N_{SC}^x = 50$ and $N^y = 121$ for p_x and p_y pairing. By a visual inspection of the gap magnitude, we can estimate the superconducting coherence length ξ to be around 15 sites for p_x pairing and 10 sites for p_y pairing, giving a coarse length scale at which we expect proximity effects to be significant.

A. p_y -wave pairing

Considering first the dark grey lines in Fig. 2(a), the T_c behaviour for p_y pairing, we first observe that by adding normal

metal (NM) layers to the SC (FM with $m = 0.0$), the gap decays monotonously with layer number in an exponential decay-like manner. This is qualitatively understood as leakage of the superconducting pairing into the adjacent NM layers, causing a draining of the electrons that are part of the superconducting condensate which decreases the “bulk” gap in the SC. As more layers are added, i.e. the NM becomes thicker, the effect of adding subsequent layers diminishes and T_c eventually saturates. Replacing the NM by a FM magnetized along z , i.e. along the spin quantization axis of the gap, this leakage is modified. The T_c vs. FM thickness retains the exponential decay characteristic, but the asymptotic T_c to which the system converges is shifted and shows a clear dependence on the spin-orientation of the pairing. This is qualitatively understood by considering the DOS in the FM. At $\mu = -0.5t$, the DOS is spin-degenerate for $m = 0.0$, but becomes spin-dependent under a non-zero exchange field. This causes an effective spin-dependent interface transmission as electrons with opposite spin have a differing density of available states to occupy in the FM. This causes the gap with spin orientation associated with the higher DOS to transmit more easily while the pairing of opposite spin electrons to a larger extent is confined to

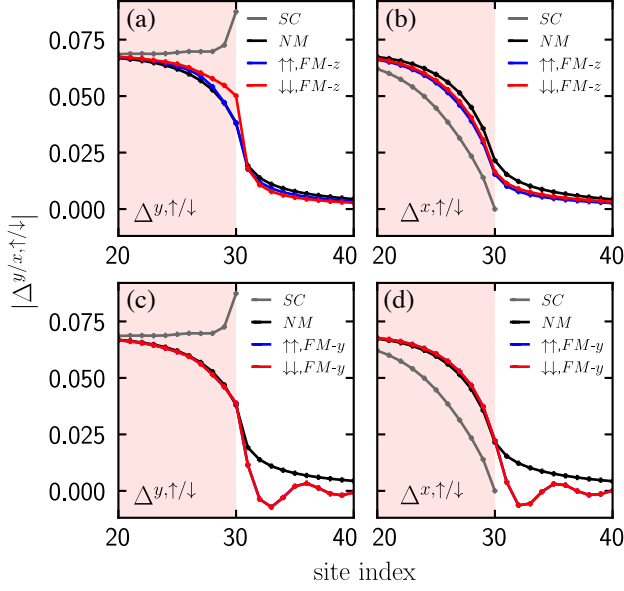


FIG. 4. Spin-up and -down gap behaviour across the SC/FM interface shown for p_y pairing in the left column (a) & (c) and p_x pairing in the right column (b) & (d). Upper row (a) & (b) shows behaviour for z -polarized FM while lower row (c) & (d) shows y -polarized FM. The grey lines denotes the gap magnitude for a bare superconductor, the pink area denotes sites in the SC. The black lines show the gap magnitude in the case of an adjacent NM while red and blue denote spin-up and down gap behaviour in the presence of FM. Data obtained using $V_x = V_y = -0.85t$, $\mu = -0.5t$ with the same geometry as in Fig. 2.

the SC interior. This is made clear in Fig. 4 where the p_y gap magnitude is shown across the SC/FM interface for a z -polarized FM in the upper left panel. Compared to the NM case (grey) which is equal for both spin orientations, there is now a clear difference between spin-up and down pairing magnitude and the extent to which they leak into adjacent layers. At $\mu = 0.0$, the FM DOS remains spin-degenerate at $E = 0.0$ also for finite exchange fields, albeit significantly lowered by the Zeeman splitting. The T_c curves for spin-up and down gap coalesce for all magnetization strengths when we approach $\mu = 0.0$. We finally point out that for the FM- z , p_y pairing case, it is possible to have a combination of exchange field strength and chemical potential which causes the spin-dependent transmission of one spin species to surpass the NM case, causing a FM-induced lowering of T_c , at least for for the pairing type which is associated with a high DOS in the FM. We note however that for chemical potentials close to half-filling, the Zeeman splitting of the DOS usually results in a reduced or comparable DOS for both spin species.

When the FM is polarized in y , the behaviour of the p_y pairing critical temperature changes significantly. Contrary to the exponential decay of the FM- z case, we now observe oscillatory behaviour of T_c as function of FM thickness which is identical for the up- and down-polarized pairing (see Fig. 4, lower left panel). If one considers the variation in exchange field strength (red curves in Fig. 2 (a)), it is also evident that

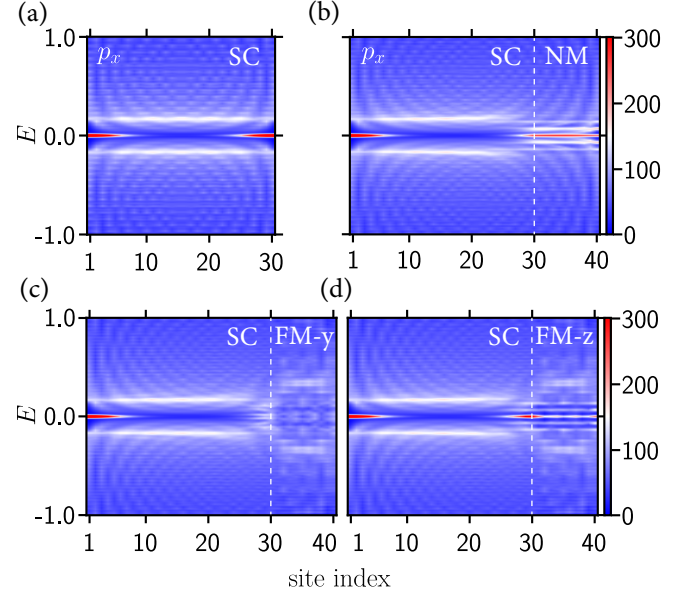


FIG. 5. LDOS for the SC/NM and SC/FM heterostructures with p_x pairing showing the isolated SC (a) and SC + 10 layers NM (b), FM- y (c) and FM- z (d), obtained using the same number of SC sites and momentum modes as in Fig. 2, but with $V_x = -1.00t$, $\mu = 0.0$ to improve clarity. (a) From the isolated SC, it is evident that mid-gap Andreev bound states form at the vacuum boundaries (left and right side of SC). (b) When adding NM layers to the SC, ABS at the SC/NM interface leaks into the adjacent layers, decreasing the presence of ABS in the SC interior. (c) In the presence of a y -polarized FM the ABS is completely absent from the SC/FM interface while we observe that in the case of z -polarized FM, the leakage of ABS is suppressed, compared to the NM case.

the oscillation frequency increases with field strength m . This behaviour is understood by recalling that as the spin quantization axis in the FM is rotated relative to the SC, the spin-up and -down gaps become non-diagonal in the new spin-basis and thus need to distribute across both spin-bands in the y -polarized FM. This gives rise to pairing with a non-zero center-of-mass momentum in the FM, giving rise to the observed oscillations. The oscillatory behaviour of the gap is shown for p_y pairing and a y -polarized FM in Fig. 4 in the lower left panel.

In other words, rotating the magnetization in-plane from z to y (e.g. with an external field) changes the qualitative behavior of T_c vs. the thickness of the FM from decaying to oscillatory. This is a unique signature of triplet pairing which would not occur either for BCS superconductors or even for high- T_c d -wave superconductors since they are still spin-singlets. In those cases, only an oscillatory decaying behavior would be seen (albeit with a long oscillation length for a weakly polarized FM). This is because spin-singlet pairs are rotationally invariant and thus do not respond differently to magnetizations in different directions. In the present case with intrinsic triplet superconductivity, this is no longer the case and rotating the magnetization causes T_c to change.

B. p_x -wave pairing: the role of Andreev bound states

Keeping in mind the essential mechanisms discussed above, we now move on to the case of p_x pairing, depicted in Fig. 2 (b). Starting with the NM case, in contrast with the behaviour of the p_y pairing, T_c is now predicted to increase as the NM thickness increases. If the NM is replaced by a FM in z , we note that the inverse exponential decay behaviour is preserved with a shifted asymptotic T_c . In order to understand the T_c behaviour, we must consider a crucial difference between p_y and p_x pairing in our system, namely that the p_x pairing, being of odd spatial symmetry and normal to the interface, is affected by the formation of Andreev bound states (ABS) at the vacuum boundary to the left in Fig. 1 as well as at the SC / FM interface [20, 21]. ABS are mid-gap states, located within the superconducting gap. In regions where ABS are prominent, the superconducting gap is suppressed. In structures of limited thickness comparable to the superconducting coherence length, we can expect this interfacial gap suppression to have an effect on the gap throughout the superconducting region, causing a reduction in the critical temperature compared to the case of p_y lacking ABS formation. With this in mind, we can now better grasp the T_c behaviour observed in Fig. 2 (b). As NM layers are added to the SC, the ABS originally confined to the SC interior of the SC / FM interface may leak into the adjacent layers, reducing their inhibitory effect on the gap in the SC. When the NM is replaced by a z -polarized FM, this relocalization of the ABS from the SC to the adjacent layers is suppressed by the reduced DOS in the FM. This is shown in Fig. 4 (b) where we observe that the gap magnitude in the SC interior increases when NM layers are added (compare the grey and black lines), an effect which to some extent is suppressed when the NM is replaced by a FM- z ($m = 1.0t$) (red and blue lines in Fig. 4 (b)). In the case of a y -polarized FM, we observe that the gap magnitude behaves like the gap in the presence of NM, but begins to oscillate in the FM, similarly as in the p_y case.

The effect of NM/FM layers on the ABS can be studied more closely by considering the LDOS, shown in Fig. 5. Here, LDOS is shown for an isolated SC as well as SC + 10 sites NM, FM- z and FM- y . From comparisons between Fig. 5(a) and (b), it follows that the presence of the NM layers suppresses ABS formation at the interface through a relocalization of the ABS into the NM layers as discussed above. Replacing the NM with a z -polarized FM (Fig. 5(d)) reduces the suppressive effect on the ABS due to reduced interface transmission. The addition of y -polarized FM layers has the opposite effect, the ABS states previously associated with the right SC boundary

are completely absent in Fig. 5(b). This can be understood by recalling that we consider equal-spin pairing. ABS formation at the SC/FM interface due to the odd spatial symmetry of the order parameter necessarily has the same spin structure and is inhibited by the introduction of spin-flip scattering by the y -polarized FM. Keeping this in mind, we can now understand why the presence of a y -polarized FM gives a T_c increase stronger than the NM case while a z -polarized FM gives an increase smaller than the NM.

Finally, we note that the effect of how the superconducting pairing symmetry affects the preferred stable magnetization direction was analyzed in [22]. In the present work, the magnetization direction is instead taken to be fixed, for instance by an internal magnetoanisotropy field which is greater than effective anisotropy induced by the superconducting state [23].

IV. CONCLUSION

We have computed the critical temperature of a superconductor with intrinsic triplet pairing that is in proximity to a thin ferromagnetic layer. We show that the dependence of T_c on the thickness N_{layers} of the ferromagnet and its in-plane magnetization orientation are determined by both the spin and orbital part of the superconducting order parameter. Firstly, we find that T_c either decays monotonically or oscillatory with N_{layers} depending on the magnetization direction. This is fundamentally different from conventional BCS superconductors, where changing the in-plane magnetization direction leaves T_c invariant. Secondly, we find that T_c increases with N_{layers} when the triplet superconducting order parameter features Andreev bound-states at the interface (such as p_x -wave pairing) whereas T_c decreases with N_{layers} when the order parameter does not (such as p_y -wave pairing). Since T_c changes qualitatively depending on both the spin and orbital part of the superconducting order parameter, measurements of T_c in a triplet SC/FM bilayer can be used to identify intrinsic spin-triplet pairing which is a highly sought after property in superconducting materials.

ACKNOWLEDGMENTS

This work was supported by the Research Council of Norway through Grant No. 323766 and its Centres of Excellence funding scheme Grant No. 262633 “QuSpin”. Support from Sigma2 - the National Infrastructure for High-Performance Computing and Data Storage in Norway, project NN9577K, is acknowledged.

[1] A. I. Buzdin, *Rev. Mod. Phys.* **77**, 935 (2005).
[2] F. S. Bergeret, A. F. Volkov, and K. B. Efetov, *Rev. Mod. Phys.* **77**, 1321 (2005).
[3] F. S. Bergeret, A. F. Volkov, and K. B. Efetov, *Phys. Rev. Lett.* **86**, 4096 (2001).
[4] R. S. Keizer, S. T. B. Goennenwein, T. M. Klapwijk, G. Miao, and A. Gupta, *Nature* **439**, 825 (2006).

[5] T. S. Khaire, M. A. Khasawneh, W. P. Pratt, and N. O. Birge, *Phys. Rev. Lett.* **104**, 137002 (2010).
[6] J. W. A. Robinson, J. D. S. Witt, and M. G. Blamire, *Science* **329**, 59 (2010).
[7] M. Eschrig, *Rep. Prog. Phys.* **78**, 104501 (2015).
[8] J. Linder and J. W. A. Robinson, *Nat. Phys.* **11**, 307 (2015).

- [9] S. S. Saxena, P. Agarwal, K. Ahilan, F. M. Grosche, R. K. W. Haselwimmer, M. J. Steiner, E. Pugh, I. R. Walker, S. R. Julian, P. Monthoux, G. G. Lonzarich, A. Huxley, I. Sheikin, D. Braithwaite, and J. Flouquet, [Nature](#) **406**, 587–592 (2000).
 - [10] D. Aoki, A. Huxley, E. Ressouche, D. Braithwaite, J. Flouquet, J.-P. Brison, E. Lhotel, and C. Paulsen, [Nature](#) **413**, 613–616 (2001).
 - [11] D. Aoki, F. Hardy, A. Miyake, V. Taufour, T. D. Matsuda, and J. Flouquet, [C. R. Physique](#) **12**, 573 (2011).
 - [12] N. T. Huy, A. Gasparini, D. E. de Nijs, Y. Huang, J. C. P. Klaasse, T. Gortenmulder, A. de Visser, A. Hamann, T. Görlach, and H. v. Löhneysen, [Phys. Rev. Lett.](#) **99**, 067006 (2007).
 - [13] C. Cirillo, S. L. Prischepa, M. Salvato, C. Attanasio, M. Hesselberth, and J. Aarts, [Phys. Rev. B](#) **72**, 144511 (2005).
 - [14] V. Zdravkov, A. Sidorenko, G. Obermeier, S. Gsell, M. Schreck, C. Müller, S. Horn, R. Tidecks, and L. R. Tagirov, [Phys. Rev. Lett.](#) **97**, 057004 (2006).
 - [15] P. V. Leksin, N. N. Garif'yanov, I. A. Garifullin, Y. V. Fominov, J. Schumann, Y. Krupskaya, V. Kataev, O. G. Schmidt, and B. Büchner, [Phys. Rev. Lett.](#) **109**, 057005 (2012).
 - [16] Y. Gu, J. W. A. Robinson, M. Bianchetti, N. A. Stelmashenko, D. Astill, F. M. Grosche, J. L. MacManus-Driscoll, and M. G. Blamire, [APL Materials](#) **2**, 046103 (2014).
 - [17] J. A. Ouassou, *Density of states and critical temperature in superconductor/ferromagnet structures with spin-orbit coupling*, Master's thesis, NTNU (2015).
 - [18] L. G. Johnsen, K. Svalland, and J. Linder, [Phys. Rev. Lett.](#) **125**, 107002 (2020).
 - [19] A. P. Mackenzie and Y. Maeno, [Rev. Mod. Phys.](#) **75**, 657 (2003).
 - [20] C.-R. Hu, [Phys. Rev. Lett.](#) **72**, 1526 (1994).
 - [21] Y. Tanaka and S. Kashiwaya, [Phys. Rev. Lett.](#) **74**, 3451 (1995).
 - [22] P. Gentile, M. Cuoco, A. Romano, C. Noce, D. Manske, and P. M. R. Brydon, [Phys. Rev. Lett.](#) **111**, 097003 (2013).
 - [23] L. G. Johnsen, N. Banerjee, and J. Linder, [Phys. Rev. B](#) **99**, 134516 (2019).
-

Appendix A: p -wave term in mean field theory

We consider now the nearest-neighbour attractive interaction modelled by the term

$$\sum_{\langle i,j \rangle, \sigma} V_{ij} n_{i, \sigma} n_{j, \sigma} \quad (\text{A1})$$

in the Hamiltonian. We assume now that the site coordinate carries two components, $i = (i_x, i_y)$ where x is the direction normal to the interface and y the parallel direction. We may then introduce Fourier-transformed operators in the latter direction in order to take full advantage of the periodicity of the system. We proceed by rewriting the Hamiltonian using these transformed operators, assuming the attractive interaction to be isotropic, $V_{ij} = V \leq 0$.

$$\sum_{\langle i,j \rangle, \sigma} V_{ij} n_{i, \sigma} n_{j, \sigma} = V \sum_{(i_x, i_y), \delta, \sigma} n_{(i_x, i_y), \sigma} n_{(i_x + \delta_x, i_y + \delta_y), \sigma} \quad (\text{A2})$$

$$= V \sum_{(i_x, i_y), \delta, \sigma} c_{(i_x, i_y), \sigma}^\dagger c_{(i_x, i_y), \sigma} c_{(i_x + \delta_x, i_y + \delta_y), \sigma}^\dagger c_{(i_x + \delta_x, i_y + \delta_y), \sigma} \quad (\text{A3})$$

where $\delta_{x/y}$ are the x and y components of the nearest neighbour vector. We now introduce Fourier-transformed operators in the y direction:

$$V \sum_{(i_x, i_y), \delta, \sigma} c_{(i_x, i_y), \sigma}^\dagger c_{(i_x, i_y), \sigma} c_{(i_x + \delta_x, i_y + \delta_y), \sigma}^\dagger c_{(i_x + \delta_x, i_y + \delta_y), \sigma} \quad (\text{A4})$$

$$= \frac{V}{(N^y)^2} \sum_{(i_x, i_y), \delta, \sigma} \sum_{k_y^1, k_y^2, k_y^3, k_y^4} c_{i_x, k_y^1, \sigma}^\dagger c_{i_x, k_y^2, \sigma} c_{i_x + \delta_x, k_y^3, \sigma}^\dagger c_{i_x + \delta_x, k_y^4, \sigma} e^{-i(k_y^1 - k_y^2 + k_y^3 - k_y^4) r_{i_y}} e^{-i(k_y^3 - k_y^4) \delta_y} \quad (\text{A5})$$

$$= \frac{V}{N^y} \sum_{i_x, \delta, \sigma} \sum_{k_y^2, k_y^3, k_y^4} c_{i_x, k_y^2 - k_y^3 + k_y^4, \sigma}^\dagger c_{i_x, k_y^2, \sigma} c_{i_x + \delta_x, k_y^3, \sigma}^\dagger c_{i_x + \delta_x, k_y^4, \sigma} e^{-i(k_y^3 - k_y^4) \delta_y} \quad (\text{A6})$$

Renaming the momentum variables now as $k_y^2 = k$, $k_y^4 = k'$ and $k_y^3 = k' - q$, ignoring the y subscripts from now on, we may rewrite the above as

$$\frac{V}{N^y} \sum_{i_x, \delta, \sigma} \sum_{k, k', q} c_{i_x, k+q, \sigma}^\dagger c_{i_x, k, \sigma} c_{i_x + \delta_x, k' - q, \sigma}^\dagger c_{i_x + \delta_x, k', \sigma} e^{iq \delta_y} \quad (\text{A7})$$

$$= \frac{V}{N^y} \sum_{i_x, \delta, \sigma} \sum_{k, k', q} c_{i_x + \delta_x, k' - q, \sigma}^\dagger c_{i_x, k+q, \sigma} c_{i_x, k, \sigma} c_{i_x + \delta_x, k', \sigma} e^{iq \delta_y} \quad (\text{A8})$$

We now proceed by using that the attractive interaction only facilitates scattering between states located in a thin shell around the Fermi surface. By considering the kinematics, it follows that the scattering phase space is maximized by considering the case where $k' = -k$. In the following, we shall keep only such terms. We can then rewrite the expression as

$$\frac{V}{N^y} \sum_{i_x, \delta, \sigma} \sum_{k, q} c_{i_x + \delta_x, -k - q, \sigma}^\dagger c_{i_x, k+q, \sigma} c_{i_x, k, \sigma} c_{i_x + \delta_x, -k, \sigma} e^{iq \delta_y} \quad (\text{A9})$$

$$= \frac{V}{N^y} \sum_{i_x, \delta, \sigma} \sum_{k, k'} c_{i_x + \delta_x, -k', \sigma}^\dagger c_{i_x, k', \sigma} c_{i_x, k, \sigma} c_{i_x + \delta_x, -k, \sigma} e^{i(k' - k) \delta_y} \quad (\text{A10})$$

where we have introduced a final variable $k' = k + q$. We now introduce the mean fields $\langle c_{i_x + \delta_x, -k', \sigma}^\dagger c_{i_x, k', \sigma} \rangle$, $\langle c_{i_x, k, \sigma} c_{i_x + \delta_x, -k, \sigma} \rangle$ and rewrite the above to first order in the deviation from the mean fields,

$$\frac{V}{N^y} = \sum_{i_x, \delta, \sigma} \sum_{k, k'} c_{i_x + \delta_x, -k', \sigma}^\dagger c_{i_x, k', \sigma} c_{i_x, k, \sigma} \langle c_{i_x, k, \sigma} c_{i_x + \delta_x, -k, \sigma} \rangle e^{i(k' - k) \delta_y} + \text{h.c.} \quad (\text{A11})$$

$$= \sum_{i_x, \sigma} \sum_k c_{i_x + \hat{x}, -k, \sigma}^\dagger c_{i_x, k, \sigma} \Delta_i^{\sigma, \hat{x}} + c_{i_x - \hat{x}, -k, \sigma}^\dagger c_{i_x, k, \sigma} \Delta_i^{\sigma, -\hat{x}} + c_{i_x, -k, \sigma}^\dagger c_{i_x, k, \sigma} \Delta_k^{\sigma, \hat{y}} + \text{h.c.} \quad (\text{A12})$$

where we have defined the gaps

$$\Delta_i^{\sigma, \pm \hat{x}} = \frac{V_x}{N^y} \sum_{k'} F_{i, k'}^{\sigma, \pm \hat{x}} \quad (\text{A13})$$

$$\Delta_{i, k}^{\sigma, \hat{y}} = \frac{V_y}{N^y} \sum_{k'} 2 \cos(k' - k) F_{i, k'}^{\sigma, \hat{y}}, \quad (\text{A14})$$

and the pairing amplitudes

$$F_{i,k'}^{\sigma,\pm\hat{x}} = \langle c_{i,k',\sigma} c_{i\pm\hat{x},-k',\sigma} \rangle \quad (\text{A15})$$

$$F_{i,k'}^{\sigma,\hat{y}} = \langle c_{i,k',\sigma} c_{i,-k',\sigma} \rangle, \quad (\text{A16})$$

We can now write the contribution to the Hamiltonian from the p -wave coupling as

$$H = E_0 + \frac{1}{2} \sum_{i_x, j_x} B_{i_x}^\dagger h_{i_x, j_x} B_{j_x} \quad (\text{A17})$$

where we have for $i_x = j_x$,

$$h_{i_x, i_x} = \sum_k \begin{pmatrix} c_{i_x, k, \uparrow}^\dagger \\ c_{i_x, k, \downarrow}^\dagger \\ c_{i_x, -k, \uparrow} \\ c_{i_x, -k, \downarrow} \end{pmatrix}^T \begin{bmatrix} 0 & 0 & -2\Delta_{i,k}^{\uparrow, \hat{y}} & 0 \\ 0 & 0 & 0 & -2\Delta_{i,k}^{\downarrow, \hat{y}} \\ -2(\Delta_{i,k}^{\uparrow, \hat{y}})^\dagger & 0 & 0 & 0 \\ 0 & -2(\Delta_{i,k}^{\downarrow, \hat{y}})^\dagger & 0 & 0 \end{bmatrix} \begin{pmatrix} c_{i_x, k, \uparrow} \\ c_{i_x, k, \downarrow} \\ c_{i_x, -k, \uparrow}^\dagger \\ c_{i_x, -k, \downarrow}^\dagger \end{pmatrix} \quad (\text{A18})$$

and $j_x = i_x \pm \hat{x}$,

$$h_{i_x, i_x \pm \hat{x}} = \sum_k \begin{pmatrix} c_{i_x, k, \uparrow}^\dagger \\ c_{i_x, k, \downarrow}^\dagger \\ c_{i_x, -k, \uparrow} \\ c_{i_x, -k, \downarrow} \end{pmatrix}^T \begin{bmatrix} 0 & 0 & -2\Delta_i^{\uparrow, \pm\hat{x}} & 0 \\ 0 & 0 & 0 & -2\Delta_i^{\downarrow, \pm\hat{x}} \\ 2(\Delta_i^{\uparrow, \pm\hat{x}})^\dagger & 0 & 0 & 0 \\ 0 & 2(\Delta_i^{\downarrow, \pm\hat{x}})^\dagger & 0 & 0 \end{bmatrix} \begin{pmatrix} c_{i_x \pm \hat{x}, k, \uparrow} \\ c_{i_x \pm \hat{x}, k, \downarrow} \\ c_{i_x \pm \hat{x}, -k, \uparrow}^\dagger \\ c_{i_x \pm \hat{x}, -k, \downarrow}^\dagger \end{pmatrix} \quad (\text{A19})$$
